Autonomous Acoustic-Aided Optical Localization for Data Transfer

Johanna Hansen[1], Dehann Fourie[2], James C. Kinsey[1], Clifford Pontbriand[1], John Ware[1], Norm Farr[1], Carl L. Kaiser[1], and Maurice Tivey[3]

***Abstract*— The emergence of high speed optical communication systems has introduced a method for transferring data relatively quickly underwater. This technology coupled with autonomous underwater vehicles (AUVs) has the potential to enable efficient wireless data transfers underwater. Data muling, a data transport mechanism in which AUVs visit remote sensor nodes to transfer data, enables remote data to be recovered cheaply from underwater sensors. This paper details efforts to develop a system to reduce operational complexities of autonomous data-muling.**

We report a set of algorithms, systems, and experimental results of a technique to localize a sub-sea sensor node equipped with acoustic and optical communication devices with an AUV. Our homing system was designed to utilize the long-range, low-power acoustic signal to determine the sensor location from great distances. When within optical communication range, it exploits the optical power pattern to center the vehicle over the sensor node for optimum data transfer. These implementations were tested over three dives at varying levels of automation. Data collected from the real-time system has been tested in full-automation mode within our simulation environment.

I. Introduction

In-situ deep ocean observing sensors often independently collect information that must be retrieved for analysis. Retrieving this data is a costly process, especially if the sensor must be brought to surface for data download and redeployment. An option to reduce operational expense associated with retrieving deep-ocean data is to offload the data at depth with a robotic vehicle. New optical communication technologies enable this concept, known as data-muling, by providing underwater wireless transfer rates with speeds approaching $400\ Mbps$ at close range [1].

Woods Hole Oceanographic Institution (WHOI) demonstrated data-muling with the *Sentry* autonomous underwater vehicle (AUV) [2] equipped with a WHOI omni-directional optical modem as reported in Pontbriand *et al.*. In [1], Pontbriand showed that data transfer increase as distance between optical modems decrease. This makes a compelling case for developing an AUV capability in which it is able to adaptively minimize distance to an optical modem during a data-muling task. This requires behavioral responses from the AUV which extend beyond pure way-point following navigation schemes typically employed by many operational AUVs, including *Sentry*.

In this paper we discuss optimizing optical data-muling for busy AUV operations. We explore a method to reduce operational complexity while also improving optical data transfer speeds by extending the AUV's autonomy. With this system, we are able to relax preemptive geolocation requirements of a sensor deployed to the seafloor by allowing the AUV to navigate to the sensor autonomously.

We exploit data transfer synergies between a low-power, low-bandwidth, long-range acoustic channel and high bandwidth, short-range optical channel [3], [4]. Our method implies a high premium on robustness of the control strategies used, since vehicle actions cannot be known in advance and will depend on the situation encountered in the field. Simulation and validation are therefore key enablers in the development of behavioral control strategies.

The remainder of this paper is organized as follows: Related work is briefly discussed in Section II. Section III outlines our technical approach, specifically the acoustic and optical homing to a node on the sea floor. We discuss integration with the AUV *Sentry* and design considerations in Section IV. Performance analysis and validation from simulation and field trial data are presented Section V.

II. Background

Underwater optical communication has been demonstrated since the 1990s [5], but early systems possessed limited range ($\sim 20\ m$). Since then, the range of operation has been increased to approximately $100\ m$, with much higher data rates possible [1], [3], [4], [6], [7].

Data muling, a process of harvesting data from remote sensors, can benefit greatly from wireless optical communications and has previously been studied by [4], [8], [9]. One challenge with a data mule is placing the mule in close enough proximity to a deployed optical modem for sustained high-speed data transfer.

Classic approaches, such as that used in [8], utilize high quality absolute global location information of both the mule and deployment to determine the relative distance between the two. This approach often becomes prohibitively expensive, considering the high quality navigation equipment (e.g., long-baseline (LBL) or ultra-short baseline (USBL)) required to locate the lander and program an AUV to navigate to that same location. Furthermore, the mission control software of many AUVs follows a non-behavioral architecture, which minimizes risk by stipulating an underwater mission execution time-line [10]. Such strict control architectures prohibit the vehicle from dynamically changing the mission plan on the fly. In the case of acousto-optical relative navigation, the necessary information only becomes available as the vehicle is performing its mission in real-time.

Doniec *et al.* [9] demonstrated an acousto-optical search system to discover (PANDA) sensor nodes at distances of $25\ m$ and $100\ m$ using the Autonomous Modular Optical

978-0-933957-43-5 ©2015 MTS

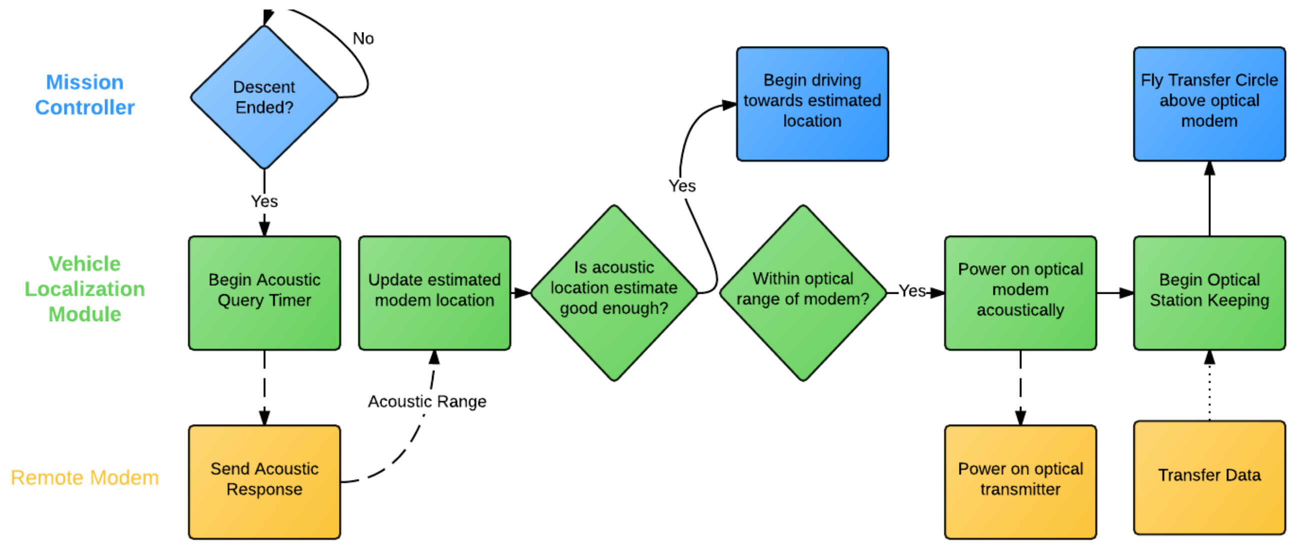

Fig. 1. Acousto-optical localization logic and considerations. Control, localization, and modem control and reporting are contained within blue, green, and orange, respectively. Ethernet communication is contained within the vehicle and is denoted by a solid line. Acoustic and optical communications are external to the vehicle and are denoted by dashed and dotted lines, respectively.

Underwater Robot (AMOUR). This system utilized gradient descent along with a particle filter to adaptively search for the acoustic signal. The vehicle mission would then be updated without precise global position information of the deployed node. To our knowledge, deep ocean adaptive localization of and navigation to an acousto-optic deployment, followed by data transfer from it, has not been demonstrated before.

This work presents further investigation of autonomous control and relative navigation to a deployed node for data mule applications. Furthermore, we are not aware of work using received optical power measurements to help guide the vehicle closer to an optimal data transfer trajectory.

III. Technical Approach

This work describes the system developed to optimize data transfer rates of an acousto-optic node deployed to the seafloor with only an approximate knowledge of its location. We use a robust acoustic localization method to locate the target deployment and then guide the AUV towards it from kilometers away. After arriving within optical communications range, we optimize the AUV's location based on measured optical power to improve data-transfer rate.

At a high-level, the localization and optimization procedure consists of the following steps (Figure 1):

1) Before deployment, the AUV is pre-programmed to navigate from the deployed location to an human estimated lander position on the seafloor. Several data-transfer circle tracklines are programmed at constant altitude above the estimated lander location.
2) Upon reaching dive altitude, the AUV begins sending acoustically queries to the lander for range while driving the pre-programmed tracklines.
3) The acoustic homing algorithm calculates the observed location of the lander based on several acoustic range measurements from distinct locations of the AUV.
4) The homing algorithm shifts the pre-programmed mission to position the transfer circles on top of the observed lander position after meeting a set confidence in its location estimate.
5) As the vehicle approaches the lander, it sends an acoustic command to power on the optical modem. Data transfer begins whenever the optical link is available.
6) The vehicle begins flying a tight optical transfer circle above the modem.
7) The optical station-keeping algorithm slowly shifts the center point of the the optical transfer circle based on measured optical power to optimize data transfer rate.

A. Acoustic Localization

The first stage of the system (upon reaching the desired altitude above the seafloor) consists of localizing the position of the sensor node via acoustic ranging. It is well established that a range estimate can be made by measuring the time of flight of a signal between two beacons [11], [12], [13]. In our scenario, the AUV observes acoustic messages to the fixed beacon from spatially distinct locations to constrain the relative position of lander. Range is computed by an AvTrak 6 acoustic modem [14] based on the round-trip time of flight of the message and the speed of sound in water.

In developing the localization scheme, we utilize a statistical approach to improve robustness and reduce susceptibility to noise. To compute the lander location acoustically, we assume that the depth of the lander is known, D_L, and the depth of the vehicle at each point, D_N, is known. This allows the projection of the observed range, R_N, to a range in the 2D coordinate space, r_N, as described by Equation 1 in [12].

$$r_N = \sqrt{R_N^2 - (D_L - D_N)^2} \quad (1)$$

For each range measurement at an AUV position, there is a maximum of two intersections with every previous range measurement.

$$2(x_2 - x_1)x + 2(y_2 - y_1)y = r_1^2 - x_1^2 - y_1^2 - r_2^2 + x_2^2 + y_2^2 \quad (2)$$

We utilize the intersections of all of the observed circles to develop a list of intersecting points using Equation 2. In a zero-noise scenario, all circles will intersect at the location of the lander. However, we realize that this is unlikely in a real system. To locate the position with the most intersection points, we round x, y, to the nearest meter and add them to a location bin described as a grid, $I(x, y)$.

$$G = \sum I(x - u, y - v)g(u, v)_{u,v} \quad (3)$$

We then perform a 2D convolution where I is the grid space and g is a 10×10 array of ones, giving G. $M = max(G)$ then gives a $10x10\ m$ region where the most intersection circles are found. We then return to the original intersection values and calculate medians of x and y, bounded by M. These median values are declared the calulated lander location, with error determined as $count(M)/count(intersections)$.

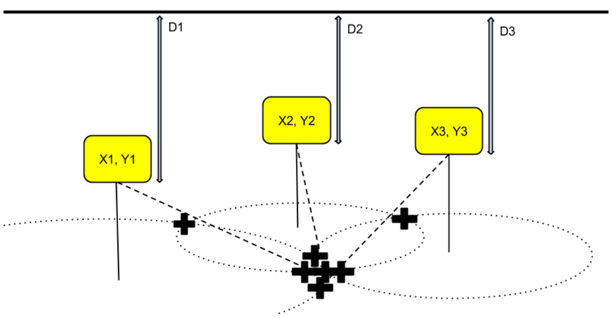

Fig. 2. Possible lander locations at observation, n.

The number of measurements needed to localize a beacon is strongly dependent on the path specified in the mission plan. Straight AUV trajectories are the worst possible case [11]. Better performance was found in simulation by varying the X and Y directions separately, thereby constructing a good multi-view baseline.

B. Optical Station Optimization

Sea trials have shown a reliable increase in optical power as the range between optical transponders decreases, producing monotonic hemispherical optical power pattern around the transponder [1]. The station-optimization algorithm exploits this prior knowledge to improve transfer speed. To enable data transfer, the AUV is flown in a tight circular pattern at a constant altitude over the optical modem. The algorithm splits the transfer circle into eight sectors, delineated by vehicle heading. As the vehicle circumnavigates the transfer circle above the lander, optical power is measured and the value at each point is added to a running average of valid power measurements of the current sector.

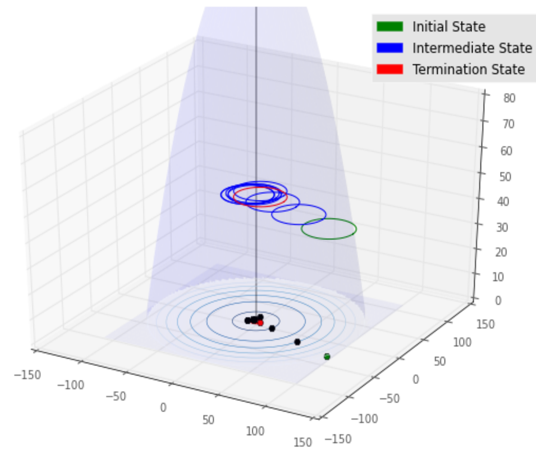

Fig. 3. Optical station-keeping optimizes data-transfer circle based on measured optical power (simulated). The blue shaded surface represents the outer bound of measurable optical power, based on field data section V-B; circles represent a data collection loop traveled by the AUV, dots on the ground represent the center of the circle in the navigation frame, and the concentric contours represent the achievable data rates.

After each complete loop, an adjustment, d, is made to the center of the next circle. The center shift is computed by stepping into the sector that measured the the highest optical power. The step size is determined by:

$$d = \frac{2\left(75^2\right)}{120\pi} \tan^{-1}\left[\frac{4\left(\Phi_{max} - \Phi_{min}\right) + 10}{P_{max} + 1}\right]. \quad (4)$$

Taking the difference between the highest Φ_{Max} and lowest Φ_{Min} power levels per sector decouples the expression from absolute power levels. The absolute power level at a particular range cannot be predicted in advance as it is subject to unknown variables such as water clarity or variations in manufacturing. Our approach aims to minimize sensitivity to the absolute optical power level while adjusting the center of the AUV trajectory onto the highest possible consistent power level.

For robustness, we select $75\ m$ as the maximum adjustment size; and for well matched sensitivity we use $120\ m$ as the maximum range at which any optical power can be expected. A regularization term, $+10$, is introduced to boost step size near the optimum solution, rather than ever-diminishing steps. Note the denominator is offset by 1 to prevent division by zero outside the optical power field. Centering updates could also be disabled when $\Phi_{max} - \Phi_{min}$ values have settled near zero.

Figure 3 shows ten iterations of a simulated vehicle trajectory with $25\ m$ radius loop around the initial sensor deployment estimate. Significant optical noise and power level offsets have been introduced. The green loop is the initial condition. At the end of each loop an adjustment in the lander location estimate is calculated. The estimated lander location is then updated, as indicated by dots at the center of each loop trajectory projected to the sea floor. The process repeats until some termination condition.

This approach takes conservative steps towards the estimated center of the optical power field pattern, but is able to repeatedly center successfully even if only a single optical power reading is made during the initial loops. Second, the step size is reduced as Φ_{max} and Φ_{min} become more balanced. Use of the arc-tangent function together with a maximum step size parameter prevent large spurious steps that may occur with gradient ascent methods, [9], operating on noisy or outlier data.

The optical homing algorithm further relaxes acoustic localization accuracy constraints. The approach would conceivably allow for low frequency acoustics, which operate over a longer range but have lower range resolution, to be used and still achieve maximum data transfer rates once optical power can be detected. This approach is also advantageous in the cases where the optimum power level is not directly above the modem, such as in rough terrain.

IV. System Description

System integration and testing on an operational AUV is a challenge. Testing at depth was not an option, so developing a robust simulation platform was important for the success of the demonstration as well as the safety of the vehicle.

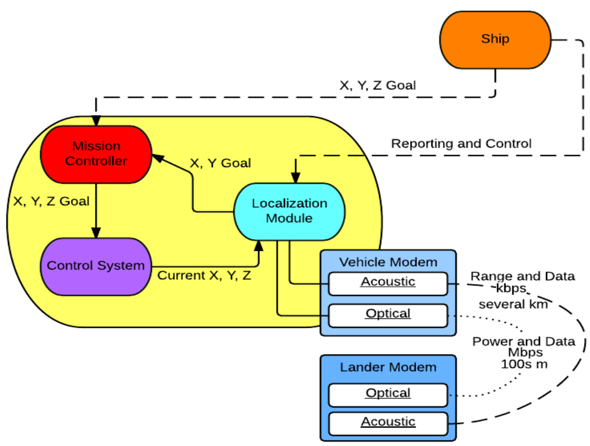

Fig. 4. System architecture on the *Sentry* AUV coupled with an acousto-optical modem. Ethernet communication is contained within the vehicle and is denoted by a solid line. Acoustic and optical communication are external to the vehicle and are denoted by dashed and dotted lines, respectively.

A. The Localization Control Module

A lightweight driver external to the vehicle's main control software, the localization module, was developed to control communications and logic among the vehicle control code, the vehicle mission controller, topside communication, and the optical acoustic system. This allowed the system to be developed quickly outside larger mission critical systems and enabled flexible testing. The localization module enabled full command of the optical/acoustic system from the ship through an existing acoustic link to the vehicle and allowed autonomy to be integrated into the system as it developed.

B. Navigation and Control

A key part of risk mitigation was building the system to externally interface with *Sentry's* mission controller without modification [10]. The mission controller executes a mission script that includes a predefined set of tracklines. A trackline consists of a start and end point specified in the Cartesian coordinate system. To enable semi-adaptive path planning within this paradigm, we utilize a function built into the mission controller that allows for the entire set of tracklines to be translated by a defined offset, Xs, Ys. This function allows the localization module to adjust the pre-defined tracklines mid-dive, enabling it to effectively steer the vehicle so that the data-transfer circles occur over the calculated lander position.

A predefined mission for an optical data transfer is typically a line from the deployment site to the estimated location of the lander, and then a data transfer region consisting of many small circles at a constant altitude above the lander. Although hovering in the data transfer region is a capability and may be desirable, we chose to maintain forward movement for the data transfer.

C. Enabling Hardware

The set-up consists of a vehicle system and a lander system that each contain an optical modem and an acoustic modem. A paired system of Sonardyne AvTrak 6 provides the acoustic communication infrastructure at 19-34 kHz, providing a range precision of $15\ mm$ [14]. The unit operates an omnidirectional system with flexible configuration. For field trials, the vehicle system was mounted on the underside of *Sentry* facing downward. The lander system was mounted facing upward, on a battery-powered lander that was independently deployed to the seafloor. This system is further described in [1].

D. Simulation Environment

We are able to fully simulate dives, both on and off the vehicle, with a full experimental suite that included the AUV's mission controller and control software [10]. The simulation environment reads the AUV's location provided on the vehicle network by the control system. The simulator then calculates an acoustic range and optical power based on the AUV range to a simulated lander location. Noise can be injected into each signal, and the lander location can be randomly generated or set manually. The random lander location generator allows the mission to be run automatically for batch testing and performance analysis (e.g, quantifying accuracy).

This simulation environment was incorporated with an existing vehicle mission simulator in which the vehicle control system is tested with the pre-planned AUV mission[10]. Injecting the simulated lander response into this fast-time simulation allowed us to visualize vehicle response as expected in the dive for field trials under various noise and data constraints.

V. Validation

Understanding the transitions from acoustic and optical localization can help shape the design of a data muling system. Better exploitation of acoustic range and optical

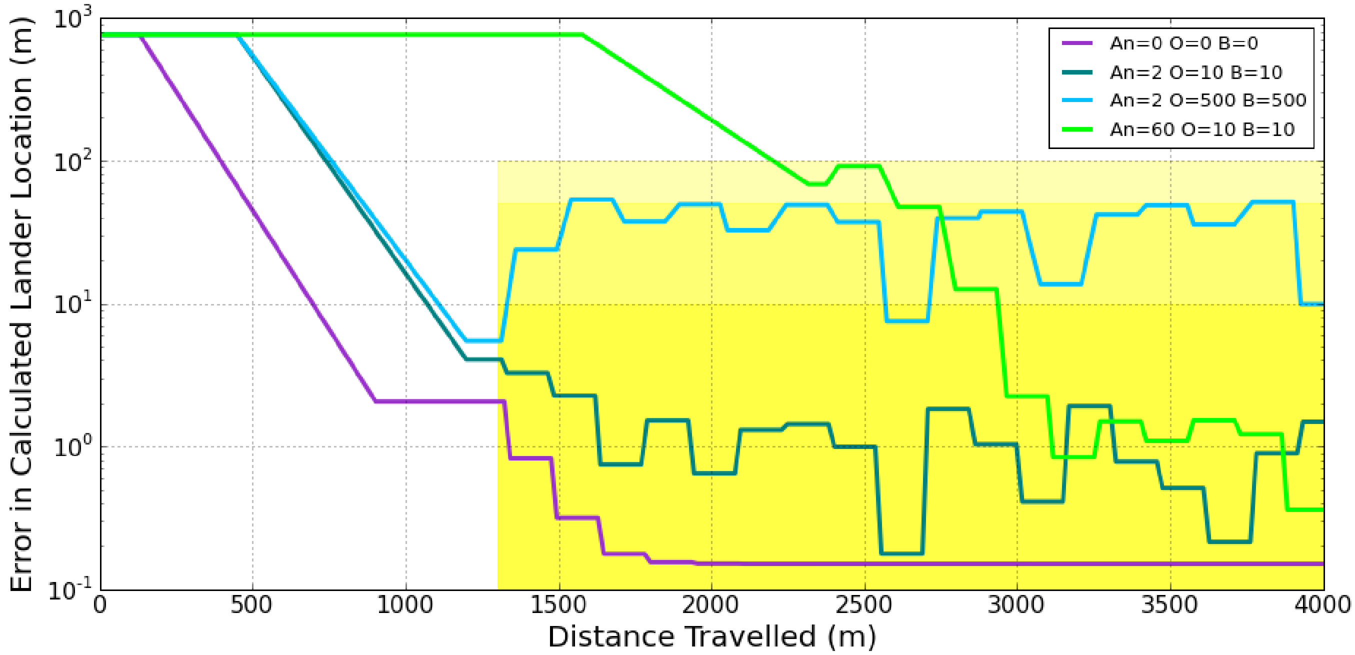

Fig. 5. Lander position estimate error in presence of various acoustic and optical noise levels, (An, O, B). The noise parameter, An, describes a multiplier of a random sample from a univariate distribution. This is added to the true calculated range to the lander. The variable O denotes the same perturbation of the simulated optical power signal. B is added simulated optical power level. The transition from acoustic localization to optical station optimization mode is indicated by the yellow shaded region. Shading in the yellow regions indicates closer proximity of the two modems and higher achievable data rates. Additional detail on this figure is in Sections IV-D and V

power measurements can ultimately help drive the cost down while ensuring a high probability of data retrieval from robotic data muling operations.

A. Simulation Analysis

The simulation allowed us to validate software communication throughout the various subsystems. It also allowed for the addition of synthetic noise that enabled us to predict system performance under various conditions. We were mainly interested in three aspects:

1) time required to converge into a stable circular trajectory above the deployed optical sensor node;
2) the accuracy with which the position of maximum optical power can be computed and maintained, given uncertainty in both the acoustic and optical power measurements; and
3) the dynamics during the transition from acoustic homing to optical homing, since we expect some tipping point interaction between acoustic and optical homing strategies.

To simulate noise, we introduce univariate normal noise into the measurements given to the localization system. The results from various noise introduction can be seen in Figure 5. To perturb the acoustic localization process, we add $An * \mathcal{N}$ to each synthetic acoustic range. Similarly, we introduce noise and bias offsets to the optical power measurements to perturb the optical station optimization algorithm. The variable O denotes the same perturbation of the simulated optical power signal and B is added simulated optical power level.

Figure 5 shows four traces of a simulated procedure that runs the acoustic and optical localization and homing strategies from a $1000\ m$ initial range. The traces represent four different cases of interest. In this simulation, acoustic ranges with various noise added were requested every $50\ m$ of travel until acoustic convergence occurred. We also sent one optical power measurement to the vehicle for each of the eight sectors in the optical-station keeping routine as the simulated vehicle flew around a data-transfer circle.

1) Accuracy of acoustic ranging vs. optical power: The violet trace in Figure 5 shows ideal performance in which perfect measurements are assumed and no additive noise is simulated. We observe that the acoustic localization algorithm determines the lander's location to within $2\ m$ after receiving four acoustic ranges with no added noise. The optical scheme localizes within $0.5\ m$ of the optimum power position.

The teal trace is representative of acoustic and optical power noise levels encountered during the field trials (discussed in Section V-B). In this case, the acoustic localization algorithm predicts the node's position to within $5\ m$, and the optical homing algorithm improves this estimate to within $1 - 2\ m$ of the optimal optical field strength.

The light blue-colored trace demonstrates the case in which optical noise is much higher than observed in field studies while the acoustic noise is held at a reasonable level. Here, we observe that the optical stabilization system is unable to shift the vehicle closer to the lander effectively. However, it does maintain the vehicle within the operating light field for data transfer.

The green trace shows the case of very high synthetic acoustic noise resulting in an imprecise value of convergence. This trace is perhaps the most significant demonstration of the value of the optical-station routine. We purposefully degrade acoustic accuracy while maintaining realistic optical noise levels. This demonstrates a scenario in which the optical algorithm can effectively improve data transfer speed by shifting the vehicle into the region of highest observed optical power. The acoustic localization scheme converges on a point that is almost $100\ m$ from the true location of the lander. However, we see that even the small amount of light observed on the edge of a transfer circle provides the optical station optimization routine with enough data to shift the vehicle in the direction of the lander and enable data transfer at maximum rate. This performances suggests that a non-acoustic paradigm in which a "lawn-mowing" survey is flown to search on optical signal alone is possible.

B. *Field Trials*

The system was tested over the course of three dives off the R/V *Atlantis* in the Juan de Fuca Ridge at depths of $1500 - 2300\ m$. The main purpose of the first dive was to produce an optical power map over the target modem as described in [1]. This was the first test of the full system at depth. Throughout the dive, the localization module enabled communication to the optical system and drove the acoustic query. It also logged power values and calculated acoustic shifts to determine the lander location, but was not allowed to send any messages to the mission controller. Instead, the calculated shifts were acoustically communicated to the ship for human approval. This dive proved the system architecture and also allowed us to develop an optical power model to use for optical stabilization [1]. The performance of the acoustic range estimates provided by the AvTrak system was more limited than expected, only reporting a valid range for distances less than 250 m. Having observed much longer range performance in previous systems, this caused us to change the power configuration settings on the system prior to the next dive.

The second dive involved an additional mapping task, completing the survey at altitudes ranging from 20 to 120 m above the lander. Throughout this dive, the localization module was allowed to automatically initiate a new data transfer whenever it detected that it was within optical power range.

A fully automated localization of the target with optical station-keeping was planned for the third dive; however, a vehicle malfunction (unrelated to the optical modem system) resulted in terminating the dive early.

VI. Conclusion

The proposed data muling system using bi-modal acousto-optical communication allows for large scale data recovery without precise *a priori* localization of the node and robot. This allows for quick deployment of *in situ* sensors with autonomous data recovery and reduces operational complexity associated with geolocating individual sensors.

This work serves as a foundation for future efforts to enable ultra long-range missions in which an AUV equipped with inexpensive navigation sensors can perform routine data collection effectively by localizing nodes acoustically. There is a tipping point in choosing the acoustic and optical system performance, which would greatly improve the probability of success for inexpensive relative navigation-based homing AUVs. The optical station-keeping can also be deployed stand-alone, allowing for optical data transfer in unknown environments by utilizing an optical grid search. This may be desirable in operational environments in which acoustic ranging is undesirable.

VII. Acknowledgments

We would like to thank the National Science Foundation whose funding through awards CE-0926849 and OCE-1036843 made this work possible. We also thank the captain and crew of the R/V *Atlantis* for their superb support of our work and the *Sentry* AUV team (Z. Berkowitz, J. Fujii, M. Lobecker) for their assistance with field operations.

References

[1] Pontbriand, C.; Farr, N.; Fourie, D.; Hansen, J.; Kinsey, J.; Pelletier, L.P; Ware, J., "Wireless Data Harvesting Using the AUV Sentry and WHOI Optical Modem," **Submitted**, OCEANS 2015.

[2] Kinsey, J.C.; Yoerger, D.R.; Jakuba, M.V.; Camilli, Rich; Fisher, Charles R.; German, C.R., "Assessing the Deepwater Horizon Oil Spill with the Sentry Autonomous Underwater Vehicle," Intelligent Robots and Systems (IROS), 2011 IEEE/RSJ International Conference on , vol., no., pp.261,267, 25-30 Sept. 2011.

[3] Farr, N.; Bowen, A.; Ware, J.; Pontbriand, C.; Tivey, M., "An Integrated, Underwater Optical /Acoustic Communications System," OCEANS 2010, vol., no., pp.1,6, 24-27 May 2010.

[4] Farr, N.E.; Ware, J.D.; Pontbriand, C.T.; Tivey, M.A., "Demonstration of Wireless Data Harvesting from a Subsea Node using a Ship of Opportunity," OCEANS 2013, vol., no., pp.1,5, 23-27 Sept. 2013.

[5] Bales, J.W.; Chryssostomos, C., "High Bandwidth, Low-power, Shot-range Optical Communication Underwater," Proc. 9th Int. Symp. on Unmanned Untethered Submersible Technology, 1995.

[6] Farr, N.; Ware, J.; Pontbriand, C.; Hammar, T.; Tivey, M., "Optical communication system expands CORK seafloor observatory's bandwidth," OCEANS 2010, vol., no., pp.1,6, 20-23 Sept. 2010.

[7] S. Harris, M. Krepel, G. Mooradian, "High-speed Blue-light Free Space Optical Receiver," IEEE SPIE. pp 9459-5

[8] Dunbabin, M.; Corke, P.; Vasilescu, I.; Rus, D., "Data Muling Over Underwater Wireless Sensor Networks Using an Autonomous Underwater Vehicle," Robotics and Automation, 2006. ICRA 2006. Proceedings 2006 IEEE International Conference on , vol., no., pp.2091,2098, 15-19 May 2006.

[9] Doniec, M.; Topor, I.; Chitre, M.; Rus, D.;, "Autonomous, Localization-Free Underwater Data Muling using Acoustic and Optical Communication," Experimental Robotics, Springer Tracts in Advanced Robotics, 2013, vol. 88. pp. 841-857.

[10] Martin, S.C.; Whitcomb, L.L.; Yoerger, D.; Singh, H., "A Mission Controller for High Level Control of Autonomous and Semi-Autonomous Underwater Vehicles," OCEANS 2006 , vol., no., pp.1,6, 18-21 Sept. 2006.

[11] Olson, E.; Leonard, J.J.; Teller, S., "Robust Range-Only Beacon Localization," Oceanic Engineering, IEEE Journal of , vol.31, no.4, pp.949,958, Oct. 2006.

[12] Newman, P.; Leonard, J., "Pure Range-only Sub-sea SLAM," Robotics and Automation, 2003. Proceedings. ICRA '03. IEEE International Conference on , vol.2, no., pp.1921,1926 vol.2, 14-19 Sept. 2003.

[13] Vaganay, J.; Baccou, P.; Jouvencel, B., ”Homing by Acoustic Ranging to a Single Beacon,” OCEANS 2000 MTS/IEEE Conference and Exhibition , vol.2, no., pp.1457,1462 vol.2, 2000.
[14] Sonardyne Avtrak 6. www.sonardyne.com. ”AvTrak 6 (Omni-Directional Version)”, March 2010.